



Re₂(CO)₆(μ-thpymS)₂ (thpymSH = pyrimidine-2-thiol) as a versatile precursor to mono- and polynuclear complexes: X-ray crystal structures of *fac*-Re(CO)₃(PPh₃)(κ²-thpymS) and two isomers of ReRu₃(CO)₁₃(μ₃-thpymS)

Md. Faruque Ahmad^a, Jagodish C. Sarker^a, Kazi A. Azam^a, Shariff E. Kabir^{a,*}, Shishir Ghosh^{a,b}, Graeme Hogarth^b, Tasneem A. Siddiquee^c, Michael G. Richmond^d

^a Department of Chemistry, Jahangirnagar University, Savar, Dhaka 1342, Bangladesh

^b Department of Chemistry, University College London, 20 Gordon Street, London WC1H 0AJ, UK

^c Department of Chemistry, Tennessee State University, 3500 John A. Merritt Blvd., Nashville, TN 37209, USA

^d Department of Chemistry, University of North Texas, 1155 Union Circle, Box 305070, Denton, TX 76203, USA

ARTICLE INFO

Article history:

Received 20 November 2012

Received in revised form

20 December 2012

Accepted 21 December 2012

Keywords:

Tetrahydropyrimidine-2-thiol

Carbonyls

X-ray structures

Mixed-metal clusters

Cluster isomerization

ABSTRACT

The dirhenium complexes Re₂(CO)₆(μ-thpymS)₂ (**1**) and *eq*-Re₂(CO)₉{κ¹-(S)-SN₂C₄H₈} (**2**) are obtained from the reaction of tetrahydropyrimidine-2-thiol (thpymSH) with Re₂(CO)₈(NCMe)₂ or Re₂(CO)₁₀. Complex **1** proves to be an excellent precursor to a range of monometallic and cluster complexes acting as a source of "Re(CO)₃(thpymS)". Thus, reactions with triphenylphosphine (PPh₃) and bis(diphenylphosphino)methane (dppm) afford mononuclear *fac*-Re(CO)₃(PPh₃)(κ²-thpymS) (**3**) and *fac*-Re(CO)₃(κ¹-dppm)(κ²-thpymS) (**4**), respectively. A crystal structure of **3** reveals that the pyrimidine-2-thiolate binds in a chelating fashion. Reactions with M₃(CO)₁₂ (M = Ru, Os) at moderate temperatures afford mixed-metal clusters. With Ru₃(CO)₁₂ in boiling thf isomeric tetranuclear butterfly clusters ReRu₃(CO)₁₃(μ₃-thpymS) (**5–6**) result which differ in the position of the capping pyrimidine-2-thiolate ligand on the cluster surface. Thus in the kinetic isomer **5**, the pyrimidine-2-thiolate caps the ReRu₂ face while in the thermodynamic isomer **6** it caps the Ru₃ face. A similar reaction with Os₃(CO)₁₀(NCMe)₂ in boiling benzene affords predominantly the ReOs₂-capped tetranuclear cluster ReOs₃(CO)₁₃(μ₃-thpymS) (**7**), together with small amounts of (μ-H)Os₃(CO)₉(μ₃-thpymS) (**8**) resulting from loss of rhenium. Cluster **7** is stable in refluxing toluene but slowly converts to isomeric **9** in xylene at 140 °C but only in low yields. The crystal structures of isomeric **5–6** have been solved and show only small variations in the cluster core geometry. Density functional calculations show that clusters **6** and **9** are slightly more stable than **5** (ΔG 2.0 kcal mol⁻¹) and **7** (ΔG 1.5 kcal mol⁻¹), respectively, and a mechanism is proposed for these conversions in which the pyrimidine-2-thiolate becomes bidentate after release of the pyrimidine group.

© 2012 Elsevier B.V. All rights reserved.

1. Introduction

Transition metal complexes bearing heterocyclic thiolato ligands (which contain nitrogen and/or sulphur as hetero atom/s) have been widely studied to understand the role of metalloproteins in biological systems [1–5] as well as being precursors for metal-sulfide materials [6–9]. Heterocyclic thiols are also attractive ligands to synthetic chemists as they are capable of coordinating to the metal centers in a variety of ways [10–20] due to the presence of both nitrogen and sulphur as potential donating atoms and

consequently the resultant complexes display a wide range of structural motifs [21–27].

We have been studying the reactivity of heterocyclic thiols with polynuclear metal carbonyls over the past few years and found that their reactivity towards polymeric carbonyls depends on both their structures and the metal carbonyls to which they are treated [1,13–20,27–36]. For instance, reactions of heterocyclic thiols with the trimetallic cluster Os₃(CO)₁₀(NCMe)₂ normally result in the oxidative addition of the S–H bond to give (μ-H)Os₃(CO)₁₀(μ-L) which decarbonylate at elevated temperature to afford (μ-H)Os₃(CO)₉(μ₃-L), whereas similar reactions with Ru₃(CO)₁₂ always afford only (μ-H)Ru₃(CO)₉(μ₃-L) [31,33]. Their reactions with Group 7 dinuclear carbonyls, M₂(CO)₁₀ (M = Re, Mn), are more diverse

* Corresponding author. Tel.: +880 27791099.

E-mail address: skabir_ju@yahoo.com (S.E. Kabir).

compared to trimetallic clusters. For example, reactions of pyridine-2-thiol (pySH) with $M_2(CO)_{10}$ ($M = Re, Mn$) give dinuclear $M_2(CO)_6(\mu-pyS)_2$ [4,26] whereas pyrimidine-2-thiol (pymSH), which contains an extra nitrogen atom in the aromatic ring, affords tetranuclear $M_4(CO)_{12}(\mu-pymS)_4$ ($M = Re, Mn$) [32]. In contrast, the five membered heterocyclic thiol, 2-mercapto-1-methylimidazole (1-MeMID), reacts with $Re_2(CO)_8(NCMe)_2$ to yield both di- and tetra- rhenium complexes, $Re_2(CO)_6(\mu-1-MeMID)_2$ and $Re_4(CO)_{12}(\mu-1-MeMID)_4$, together with the trirhenium hydride $Re_3(CO)_8(\mu-CO)(\mu-1-MeMID)_2(\mu-H)$ [18].

The reactivity of some of the resultant Group 7 di- and tetra- nuclear complexes with various mono- and bidentate ligands as well as with metal carbonyls had been investigated which reveals that they are versatile precursors for mono- and polynuclear complexes possessing $M(CO)_3(L)$ fragment [18–20,28,29]. In a continuation of our previous work on the reactivity of heterocyclic thiols with polynuclear carbonyls, we have now prepared the dirhenium complex $Re_2(CO)_6(\mu-thpymS)_2$ (**2**) and examined its reactivity towards various phosphines and polynuclear carbonyls which are the subject of this article.

2. Experimental

All manipulations were carried out under nitrogen using standard Schlenk techniques. Terahydropyrimidine-2-thiol (thpymSH), triphenylphosphine (PPh_3) and bis(diphenylphosphino) methane (dppm) were purchased from Aldrich and used as received. Metal carbonyls were purchased from Strem Chemicals Inc. and used without further purification. $Re_2(CO)_8(NCMe)_2$ and $Os_3(CO)_{10}(NCMe)_2$ were prepared according to literature methods [14,37]. Reagent-grade solvents were dried and distilled by standard methods prior to use. Infrared spectra were recorded on a Shimadzu FTIR 8101 spectrophotometer. NMR spectra were recorded on a Bruker DPX 400 instrument. Elemental analyses were performed by Wazed Miah Science Research Center, Jahangirnagar University, Dhaka. Preparative thin layer chromatography was carried out on 1 mm plates prepared from silica gel GF254 (type 60, E. Merck).

2.1. Reaction of $Re_2(CO)_{10}$ or $Re_2(CO)_8(MeCN)_2$ with thpymSH

A benzene (30 mL) solution of $Re_2(CO)_8(NCMe)_2$ (100 mg, 0.15 mmol) and thpymSH (23 mg, 0.28 mmol) was heated to reflux for 6 h. The solvent was removed under reduced pressure and the residue chromatographed by TLC on silica gel. Elution with hexane/ CH_2Cl_2 (7:3, v/v) developed three bands. The second band afforded $eq-Re_2(CO)_9(\kappa^1-S)-SN_2C_4H_8$ (**2**) (12 mg, 11%) as yellowish green crystals and the third band gave $Re_2(CO)_6(\mu-thpymS)_2$ (**1**) (36 mg, 32%) as colourless crystals after recrystallization from hexane/ CH_2Cl_2 at 4 °C. The content of the first band was too small for characterization. Alternatively, Me_3NO (63 mg, 0.84 mmol) was added dropwise to an acetone (30 mL) solution of $Re_2(CO)_{10}$ (200 mg, 0.31 mmol) and thpymSH (72 mg, 0.62 mmol) and the mixture was stirred at room temperature for 48 h. A similar workup and chromatographic separation described as above developed two bands on TLC plate which afforded **2** (12 mg, 5%) and **1** (80 mg, 34%), respectively, in order of elution.

Data for **1**: Anal. Calcd. for $C_{14}H_{14}N_4O_6Re_2S_2$: C, 21.81; H, 1.83; N, 7.27. Found: C, 22.06; H, 1.98; N, 7.40%. IR (ν_{CO} , CH_2Cl_2): 2031 m, 2006 vs, 1923 m, br cm^{-1} . 1H NMR (CD_2Cl_2): δ 5.50 (s, 2H), 3.36 (m, 8H), 1.83 (m, 4H). FAB MS (m/z): 770 (M^+).

Data for **2**: Anal. Calcd. for $C_{13}H_8N_2O_9Re_2S$: C, 21.08; H, 1.09; N, 3.78. Found: C, 21.42; H, 1.14; N, 3.86%. IR (ν_{CO} , CH_2Cl_2): 2104 m, 2023 vs, 2004 vs, 1956 m, 1915 m cm^{-1} . 1H NMR (d^6 -acetone): δ 8.51 (s, 1H), 6.64 (s, 1H), 3.65 (m, 4H), 3.26 (m, 2H). FAB MS (m/z): 740 (M^+).

2.2. Reaction of **1** with PPh_3

PPh_3 (24 mg, 0.092 mmol) was added to a CH_2Cl_2 solution (20 mL) of **1** (35 mg, 0.045 mmol) and the mixture was stirred at room temperature for 48 h. The solvent was removed under reduced pressure and the residue separated by TLC on silica gel. Elution with hexane/ CH_2Cl_2 (4:1, v/v) developed only one band which afforded $fac-Re(CO)_3(PPh_3)(\kappa^2-thpymS)$ (**3**) (32 mg, 54%) as colourless crystals after recrystallization from hexane/ CH_2Cl_2 at 4 °C.

Data for **3**: Anal. Calcd. for $C_{25}H_{22}N_2O_3ReS$: C, 46.36; H, 3.42; N, 4.33. Found: C, 46.47; H, 4.54; N, 3.46%. IR (ν_{CO} , CH_2Cl_2): 2017 vs, 1916 s, 1887 s cm^{-1} . 1H NMR ($CDCl_3$): δ 7.65 (m, 6H), 7.40 (m, 9H), 4.42 (s, br, 1H), 2.94 (m, 2H), 2.55 (m, 1H), 2.44 (m, 1H), 1.63 (m, 1H), 1.36 (m, 1H). $^{31}P\{^1H\}$ NMR ($CDCl_3$): δ 19.9 (s). FAB MS (m/z): 617 (M^+).

2.3. Reaction of **1** with dppm

To a cyclohexane (20 mL) solution of **1** (35 mg, 0.045 mmol) was added dppm (35 mg, 0.091 mmol) and the mixture was heated to reflux for 20 h. The solvent was removed under reduced pressure and the residue chromatographed by TLC on silica gel. Elution with hexane/ CH_2Cl_2 (4:1, v/v) developed three bands. The first and third bands were unconsumed dppm and **1** respectively. The second band afforded $Re(CO)_3(\kappa^1-dppm)(\kappa^2-thpymS)$ (**4**) (20 mg, 57%) as colourless crystals after recrystallization from hexane/ CH_2Cl_2 at 4 °C.

Data for **4**: Anal. Calcd. for $C_{31}H_{29}N_2O_2ReP_2S$: C, 50.19; H, 3.94; N, 3.78. Found: C, 50.30; H, 4.11; N, 3.86%. IR (ν_{CO} , CH_2Cl_2): 2016 vs, 1915 s, 1886 s cm^{-1} . 1H NMR ($CDCl_3$): δ 7.59 (m, 2H), 7.53 (m, 2H), 7.36–7.16 (m, 16H), 4.59 (s, br, 1H), 3.71 (ddd, $J = 12, 8, 4$ Hz, 1H), 3.35 (ddd, $J = 12, 8, 4$ Hz, 1H), 2.95 (m, 1H), 2.80 (dt, $J = 16, 4$ Hz, 1H), 2.56 (m, 1H), 2.06 (m, 1H), 1.51 (m, 1H), 1.01 (m, 1H). $^{31}P\{^1H\}$ NMR ($CDCl_3$): δ 11.4 (d, $J = 74.5$ Hz, 1P), –25.6 (d, $J = 74.5$ Hz, 1P). FAB MS (m/z): 742 (M^+).

2.4. Reaction of **1** with $Ru_3(CO)_{12}$

A thf (20 mL) solution of **1** (50 mg, 0.065 mmol) and $Ru_3(CO)_{12}$ (21 mg, 0.033 mmol) was heated to reflux for 30 min. The solvent was removed under reduced pressure and the residue chromatographed by TLC on silica gel. Elution with hexane/ CH_2Cl_2 (9:1, v/v) developed three bands. The first band was unconsumed $Ru_3(CO)_{12}$ and the third and second third bands gave two isomers of $ReRu_3(CO)_{13}(\mu_3-thpymS)$ (**5**, 30 mg, 24%; **6**, 10 mg, 8%) as deep red and pink crystals respectively after recrystallization from hexane/ CH_2Cl_2 at 4 °C.

Data for **5**: Anal. Calcd. for $C_{17}H_7N_2O_{13}Ru_3ReS$: C, 21.08; H, 0.73; N, 2.89. Found: C, 21.32; H, 0.95; N, 3.05%. IR (ν_{CO} , CH_2Cl_2): 2101 m, 2041 vs, 2021 m, 2007 m, 1965 m, 1910 m cm^{-1} . 1H NMR ($CDCl_3$): δ 6.76 (s, br, 1H), 4.12 (m, 2H), 3.47 (m, 2H), 2.01 (m, 2H). FAB MS (m/z): 969 (M^+).

Data for **6**: Anal. Calcd. for $C_{17}H_7N_2O_{13}Ru_3ReS$: C, 21.08; H, 0.73; N, 2.89. Found: C, 21.27; H, 0.96; N, 3.01%. IR (ν_{CO} , CH_2Cl_2): 2092 w, 2059 s, 2027 s, 2008 m, 1976 m, br. cm^{-1} . 1H NMR ($CDCl_3$): δ 6.42 (s, br, 1H), 3.57 (m, 2H), 3.36 (m, 2H), 1.94 (m, 2H). FAB MS (m/z): 969 (M^+).

2.5. Conversion of **5** to **6**

A thf (10 mL) solution of **5** (20 mg, 0.021 mmol) was heated to reflux for 2 h. A similar workup and chromatographic separation described as above furnished two bands on TLC plate. The first band gave **6** (8 mg, 40%), while the second was unconsumed **5** (3 mg).

2.6. Reaction of **1** with $\text{Os}_3(\text{CO})_{10}(\text{NCMe})_2$

To a benzene (20 mL) solution of **1** (35 mg, 0.045 mmol) was added $\text{Os}_3(\text{CO})_{10}(\text{NCMe})_2$ (22 mg, 0.026 mmol) and the mixture was refluxed for 40 min. The solvent was removed under reduced pressure and the residue chromatographed by TLC on silica gel. Elution with hexane/ CH_2Cl_2 (7:3, v/v) developed four bands. The first band was $\text{Os}_3(\text{CO})_{12}$ (trace). The second and third bands afforded (μ -H) $\text{Os}_3(\text{CO})_9(\mu_3$ -thpymS) (**8**) (8 mg, 8%) as yellow crystals and $\text{ReOs}_3(\text{CO})_{13}(\mu_3$ -thpymS) (**7**) (23 mg, 45%) as red crystals after recrystallization from hexane/ CH_2Cl_2 at 4 °C. The fourth band was too small for characterization.

Data for **7**: Anal. Calcd. for $\text{C}_{17}\text{H}_7\text{N}_2\text{O}_{13}\text{Os}_3\text{ReS}$: C, 16.52; H, 0.57; N, 2.27. Found: C, 16.77; H, 0.69; N, 2.41%. IR (ν_{CO} , CH_2Cl_2): 2107 s, 2041 vs, 2022 s, 2007 s, 1982 s, 1961 m, br, 1910 w, br. cm^{-1} . ^1H NMR (CDCl_3): δ 6.62 (s, br, 1H), 4.23 (m, 2H), 3.35 (m, 2H), 1.98 (m, 2H). FAB MS (m/z): 1236 (M^+).

Data for **8**: Anal. Calcd. for $\text{C}_{13}\text{H}_8\text{N}_2\text{O}_9\text{Os}_3\text{S}$: C, 16.63; H, 0.86; N, 2.98. Found: C, 16.82; H, 0.99; N, 3.15%. IR (ν_{CO} , CH_2Cl_2): 2083 w, 2051 vs, 2023 vs, 1994 s, 1982 sh, 1942 w, br. cm^{-1} . ^1H NMR (CDCl_3): major isomer: δ 5.79 (s, br, 1H), 3.49 (m, 2H), 3.09 (m, 2H), 1.78 (m, 2H), -15.25 (s, 1H); minor isomer: δ 5.50 (s, br, 1H), 3.35 (m, 2H), 3.13 (m, 2H), 1.68 (m, 2H), -12.44 (s, 1H). FAB MS (m/z): 939 (M^+).

2.7. Thermolysis of **7**

A xylene solution of (10 mL) of $\text{ReOs}_3(\text{CO})_{13}(\mu_3$ -thpymS) (**7**) (13 mg, 0.01 mmol) was refluxed for 1 h. The colour of the reaction mixture changed from red to pale yellow. The solvent was removed under reduced pressure and the residue was chromatographed by TLC on silica gel. Elution with hexane/ CH_2Cl_2 (7:3, v/v) developed two bands. The first band was unconsumed $\text{ReOs}_3(\text{CO})_{13}(\mu_3$ -thpymS) (**7**) (1.5 mg) and the second band gave $\text{ReOs}_3(\text{CO})_{13}(\mu_3$ -thpymS) (**9**) (1 mg, 8%) as yellow crystals after recrystallization from hexane/ CH_2Cl_2 at 4 °C.

Data for **9**: Anal. Calcd. for $\text{C}_{17}\text{H}_7\text{N}_2\text{O}_{13}\text{Os}_3\text{ReS}$: C, 16.52; H, 0.57; N, 2.27. Found: C, 16.71; H, 0.67; N, 2.36%. IR (ν_{CO} , CH_2Cl_2): 2107 w, 2094 m, 2061 vs, 2041m, 2027 vs, 2008 m, 1984 m, br. cm^{-1} .

2.8. X-ray crystallography

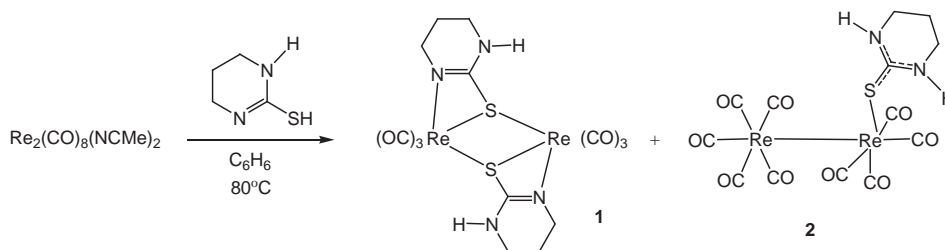
Single crystals of **3**, **5** and **6** suitable for X-ray diffraction were grown by slow diffusion of hexane into a dichloromethane solution at 4 °C. Crystallographic data was collected on a Rigaku Mercury375 R/M CCD (XtaLAB mini) diffractometer using graphite monochromated Mo-K α radiation. All calculations were carried out using the WinGX package [38] and all datasets were corrected for absorption using DIFABS [39]. The structures were solved by direct methods (SHELXS-97) [40] and refined on F^2 by full-matrix least-squares (SHELXL-97) [41] using all unique data. Non-hydrogen atoms were refined anisotropically and hydrogen atoms on C-atoms were fixed at calculated positions and refined using a riding model. Hydrogen atoms connected to N atoms were located in difference Fourier maps and refined isotropically with the N–H distances being restrained to 0.90(3) Å. All pertinent crystal data and other experimental conditions and refinement details are summarized in Table 1.

2.9. Computational methodology and modelling details

The reported calculations were performed with the hybrid DFT functional B3LYP, as implemented by the Gaussian 09 program package [42]. This functional utilizes the Becke three-parameter exchange functional (B3) [43], combined with the correlation functional of Lee, Yang and Parr (LYP) [44]. The Os, Re, and Ru atoms were described by Stuttgart–Dresden effective core potentials (ecp) and an SDD basis set, while the 6-31G(d') basis set was employed for the remaining atoms. The geometries found for clusters **5**, **6**, **7**, and **9** were fully optimized and the analytical Hessian afforded only positive eigenvalues for the ground-state

Table 1
Crystallographic data and structure refinement for **3**, **5** and **6**.

Compound	3	5	6
Empirical formula	$\text{C}_{25}\text{H}_{22}\text{N}_2\text{O}_3\text{P}_1\text{Re}_1\text{S}_1$	$\text{C}_{17}\text{H}_7\text{N}_2\text{O}_{13}\text{Ru}_3\text{ReS}$	$\text{C}_{17}\text{H}_7\text{N}_2\text{O}_{13}\text{Ru}_3\text{ReS}$
Formula weight	647.68	968.72	968.72
Temperature (K)	293(2)	293(2)	293(2)
Wavelength (Å)	0.71075	0.71075	0.71075
Crystal system	Monoclinic	Monoclinic	Monoclinic
Space group	$P 2_1/c$	$P 2_1/c$	$P 2_1/c$
Unit cell dimensions			
<i>a</i> (Å)	10.4490(8)	19.346(2)	10.231(3)
<i>b</i> (Å)	14.788(1)	9.391(1)	16.344(2)
<i>c</i> (Å)	16.173(1)	13.671(2)	15.628(2)
β (°)	101.934(7)	90.445(6)	108.84(2)
Volume (Å ³)	2445.1(3)	2483.5(5)	2473.2(8)
Z	4	4	4
Density (calculated) (Mg/m ³)	1.759	2.591	2.602
Absorption coefficient (mm ⁻¹)	5.150	6.799	6.827
<i>F</i> (000)	1264	1796	1800
Crystal size (mm ³)	0.34 × 0.21 × 0.10	0.11 × 0.08 × 0.04	0.12 × 0.11 × 0.09
θ range for data collection (°)	3.04–27.48	2.98–27.48	3.02–27.48
Index ranges	$-13 \leq h \leq 13$ $-19 \leq k \leq 19$ $-21 \leq l \leq 21$	$-25 \leq h \leq 24$ $-12 \leq k \leq 12$ $-17 \leq l \leq 17$	$-13 \leq h \leq 13$ $-21 \leq k \leq 21$ $-20 \leq l \leq 20$
Reflections collected	25,010	25,437	25,955
Independent reflections	5605 [$R(\text{int}) = 0.0545$]	5680 [$R(\text{int}) = 0.1331$]	5662 [$R(\text{int}) = 0.1086$]
Refinement method	Full-matrix least-squares on F^2	Full-matrix least-squares on F^2	Full-matrix least-squares on F^2
Max. and min. transmission	0.6269 and 0.2734	0.7727 and 0.5217	0.5786 and 0.4946
Data/restraints/parameters	5605/0/298	5680/0/334	5662/0/338
Goodness-of-fit on F^2	1.048	1.030	1.080
Final <i>R</i> indices [$I > 2\sigma(I)$]	$R_1 = 0.0292$, $wR_2 = 0.0621$	$R_1 = 0.0557$, $wR_2 = 0.0846$	$R_1 = 0.0626$, $wR_2 = 0.1368$
<i>R</i> indices (all data)	$R_1 = 0.0393$, $wR_2 = 0.0656$	$R_1 = 0.1089$, $wR_2 = 0.0971$	$R_1 = 0.1042$, $wR_2 = 0.1542$
Largest diff. peak and hole (eÅ ⁻³)	1.619 and -0.786	1.209 and -1.044	2.886 and -2.272



Scheme 1. Reaction of $\text{Re}_2(\text{CO})_8(\text{NCMe})_2$ with tetrahydropyrimidine-2-thiol.

minima. The computed frequencies were used to make zero-point and thermal corrections to the electronic energies, and the reported free energies are quoted in kcal/mol relative to the specified standard.

3. Results and discussion

3.1. Reaction of $\text{Re}_2(\text{CO})_8(\text{NCMe})_2$ or $\text{Re}_2(\text{CO})_{10}$ with *thpymSH*: formation of dirhenium complexes

Treatment of $\text{Re}_2(\text{CO})_8(\text{NCMe})_2$ with *thpymSH* in boiling benzene afforded two dirhenium complexes, namely $\text{Re}_2(\text{CO})_6(\mu\text{-thpymS})_2$ (**1**) and *eq*- $\text{Re}_2(\text{CO})_9\{\kappa^1\text{-S}\}\text{-SN}_2\text{C}_4\text{H}_8$ (**2**), in 32 and 11% yields, respectively (Scheme 1). Both were also obtained from a direct reaction between $\text{Re}_2(\text{CO})_{10}$ and *thpymSH* in the presence of Me_3NO at room temperature [yield – **1** (34%); **2** (5%)].

The target complex **1** was readily characterized by comparing its IR spectrum with similar dirhenium and dimanganese complexes [4,18,28]. The ^1H NMR spectrum shows a singlet at δ 5.50 and two multiples at δ 3.36 and 1.83 with the intensity ratio 1:4:2 which are attributable to the N–H and methylene protons of the heterocyclic ligands. The FAB mass spectrum displays a parent molecular ion at m/z 770 together with ions due to the successive loss of six carbonyls in accord with the proposed structure.

Complex **2**, a rare example of dirhenium carbonyl complexes containing a thiolato ligand coordinated in a κ^1 -fashion [45], has been characterized both spectroscopically and crystallographically [46]. The ^1H NMR spectrum displays two broad singlets at δ 8.51 and 6.64 (each integrating to 1H) attributable to the N–H protons together with two multiplets at δ 3.65 (4H) and 3.26 (2H) due to the methylene protons of the heterocyclic ring. The FAB mass spectrum exhibits a parent molecular ion at m/z 740 and other ions due to sequential loss of nine carbonyls.

3.2. Reaction of **1** with PPh_3 and *dppm*: formation of mononuclear complexes

As observed for related complexes of the type $\text{M}_2(\text{CO})_6(\mu\text{-L})_2$ ($\text{M} = \text{Re}, \text{Mn}$; $\text{L} =$ heterocyclic thiolato ligand), dirhenium **1** undergoes facile Re–S bond scission to afford mononuclear complexes when treated with phosphines. Thus reaction of **1** with PPh_3

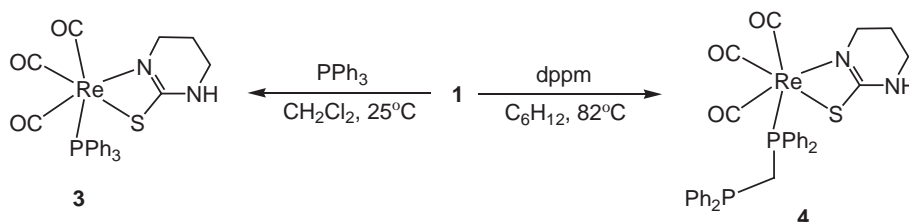
and *dppm* affords *fac*- $\text{Re}(\text{CO})_3(\text{PPh}_3)(\kappa^2\text{-thpymS})$ (**3**) and *fac*- $\text{Re}(\text{CO})_3(\kappa^1\text{-dppm})(\kappa^2\text{-thpymS})$ (**4**) in 54 and 57% yields, respectively (Scheme 2). The reaction with PPh_3 proceeded smoothly at room temperature, but addition of *dppm* was very slow under these conditions and was carried out in boiling cyclohexane. The greater reactivity of **1** towards PPh_3 as compared to *dppm* suggests that the reaction is associative in nature, with the approach of the larger diphosphine to compound **1** having a higher activation barrier.

Characterisation was relatively straightforward, the IR spectra of both showing three strong carbonyl bands characteristic of complexes containing a *fac*- $\text{Re}(\text{CO})_3$ fragment [32]. The ^{31}P NMR spectrum of **3** consists only of a singlet at δ 19.9, whilst that of **4** shows two equally intense doublets at δ 11.4 and -25.6 ($J = 74.5$ Hz). A single crystal X-ray analysis of **3**, the results of which are summarised in Fig. 1, confirms the formulation. The molecule consists of a single rhenium atom coordinated by three carbonyls, a PPh_3 ligand, and a chelating tetrahydropyrimidine-2-thiolato ligand. The carbonyls are arranged in a facial fashion and the thiolato ligand is bonded to rhenium using its exocyclic sulphur atom and sp^2 -hybridized nitrogen. The N–Re–S chelate angle is very acute [$64.05(9)^\circ$] which causes major distortion from the octahedral arrangement of ligands around rhenium. The Re–P, Re–S and Re–N bond distances are similar to those reported for related complexes [32].

3.3. Reactions of **1** with $\text{M}_3(\text{CO})_{10}\text{L}_2$ ($\text{M} = \text{Ru}, \text{Os}$; $\text{L} = \text{CO}, \text{MeCN}$): formation of mixed-metal clusters

It has been shown that the structural analogues of **1** are excellent precursors for the synthesis of tetranuclear mixed-metal clusters $\text{M}_3\text{Re}(\text{CO})_{13}(\mu_3\text{-L})$ ($\text{M} = \text{Os}, \text{Ru}$; $\text{L} =$ heterocyclic thiolato ligand) [19,20,28,29,32]. Treatment of **1** with $\text{Ru}_3(\text{CO})_{12}$ in refluxing thf afforded two isomeric tetranuclear butterfly clusters **5** and **6** in 24 and 8% yield, respectively (Scheme 3). In separate control experiments we found that cluster **5** transforms into **6** under the same conditions, while thermolysis of the latter cluster in thf results in slow decomposition which suggests that **5** is the kinetic product of this reaction.

IR spectra of **5** and **6** are very similar and the FAB mass spectrum of each exhibits a molecular ion peak at m/z 969. The ^1H NMR spectra are not particularly informative as each of them displays



Scheme 2. Reaction of $\text{Re}_2(\text{CO})_6(\mu\text{-thpymS})_2$ (**1**) with PPh_3 and *dppm*.

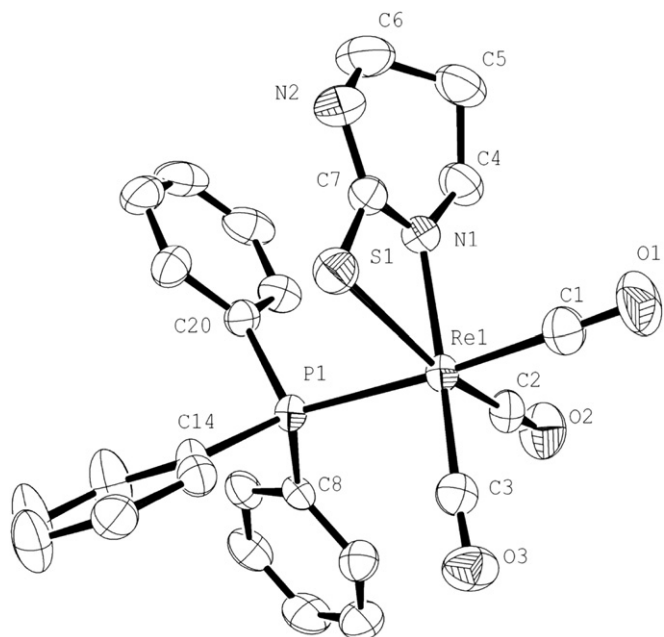


Fig. 1. X-ray structure of *fac*-Re(CO)₃(PPh₃)(κ²-thpymS) (**3**) showing the atom labelling scheme used. The hydrogen atoms are omitted for clarity. Thermal ellipsoids are drawn at 50% probability level. Selected interatomic distances (Å) and angles (°): Re(1)–P(1) 2.483(1), Re(1)–S(1) 2.554(1), Re(1)–N(1) 2.156(3), Re(1)–C(3) 1.923(4), Re(1)–C(2) 1.896(4), Re(1)–C(1) 1.940(4), N(1)–Re(1)–P(1) 89.64(9), N(1)–Re(1)–S(1) 64.05(9), P(1)–Re(1)–S(1) 84.20(3), C(7)–S(1)–Re(1) 78.5(1), C(7)–N(1)–Re(1) 105.5(3), C(4)–N(1)–Re(1) 132.9(3), N(1)–C(7)–N(2) 124.8(4), N(1)–C(7)–S(1) 112.0(3), N(2)–C(7)–S(1) 123.2(3).

four resonances attributed to the methylene and N–H protons of the pyrimidine-2-thiolato ligand. However, we were able to grow single crystals of both and carried out X-ray diffraction analyses the results of which are summarized in Figs. 2 and 3, respectively. Both products contain 62 valence electrons and exhibit a butterfly skeleton of four metal atoms with the rhenium atom at a wingtip position in both isomers. The observed four-vertex butterfly framework in **5** and **6** is consistent with Polyhedral Skeletal Electron Pair (PSEP) Theory. The metallic core is ligated by 13 carbonyls and a tetrahydropyrimidine-2-thiolato ligand that functions as a five-electron donor ligand. In both clusters, the carbonyls are all terminally bonded to the metal centers and the tetrahydropyrimidine-2-thiolato ligand is coordinated regioselectively to one of the two convex faces of the butterfly. In **5** the heterocyclic ligand caps the ReRu₂ triangle, whereas it caps the homometallic Ru₃ face in **6**; the capping of different triangular faces by the ancillary tetrahydropyrimidine-2-thiolato ligand serves as the major differentiating point of these two clusters. In both clusters, the ruthenium–ruthenium hinge is slightly shorter than the other two ruthenium–ruthenium vectors within the molecule. Movement of the tetrahydropyrimidine-2-thiolato ligand does not change the dihedral angle at the hinge vector significantly, being 159.39(3)° in **5** and reducing to 157.56(4)° in **6**. Likewise, bonding

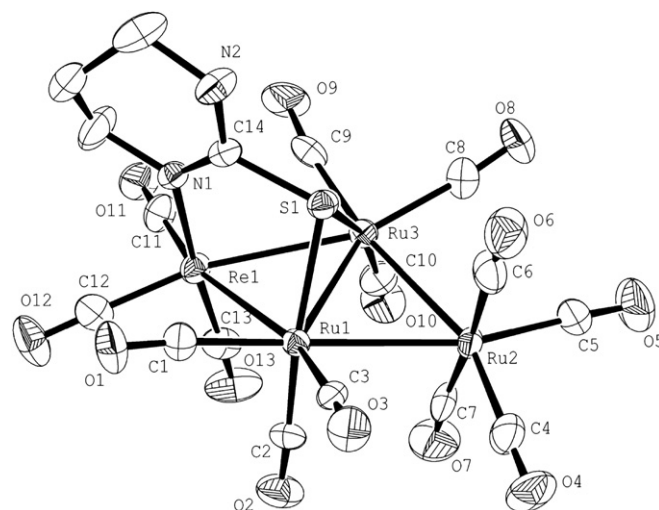
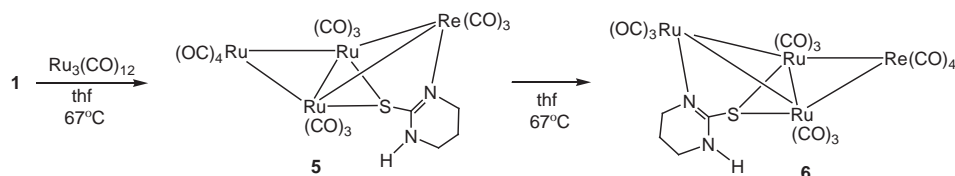


Fig. 2. X-ray structure of ReRu₃(CO)₁₃(μ₃-thpymS) (**5**) showing the atom labelling scheme used. The hydrogen atoms are omitted for clarity. Thermal ellipsoids are drawn at 50% probability level. Selected interatomic distances (Å) and angles (°): Ru(1)–Ru(2) 2.841(1), Ru(1)–Ru(3) 2.760(1), Ru(2)–Ru(3) 2.847(1), Re(1)–Ru(1) 2.9131(9), Re(1)–Ru(3) 2.922(1), Re(1)–N(1) 2.189(7), Ru(1)–S(1) 2.380(3), Ru(3)–S(1) 2.380(3), N(1)–Ru(1)–Ru(1) 85.1(2), N(1)–Re(1)–Ru(3) 84.9(2), Ru(1)–Re(1)–Ru(3) 56.47(2), S(1)–Ru(1)–Ru(3) 54.55(6), S(1)–Ru(1)–Ru(2) 81.81(7), Ru(3)–Ru(1)–Ru(2) 61.08(3), S(1)–Ru(1)–Re(1) 81.09(6), Ru(3)–Ru(1)–Re(1) 61.92(2), Ru(2)–Ru(1)–Re(1) 119.69(3), Ru(1)–Ru(2)–Ru(3) 58.06(3), S(1)–Ru(3)–Ru(1) 54.56(6), S(1)–Ru(3)–Ru(2) 81.67(6), Ru(1)–Ru(3)–Ru(2) 60.86(3), S(1)–Ru(3)–Re(1) 80.92(6), Ru(1)–Ru(3)–Re(1) 61.61(3), Ru(2)–Ru(3)–Re(1) 119.19(3), Ru(3)–S(1)–Ru(1) 70.89(7).

parameters of these isomeric clusters are very similar to each other and are within the range reported for related compounds [19,20,28].

Isomer **5** is clearly the kinetic product of the reaction, being converted into the thermodynamically more stable **6**. In order to probe the relative energy differences between the two we have carried out density functional studies on both, and we find a free energy difference of 2.0 kcal mol^{−1} in favour of cluster **6** that is in keeping with the control experiments. The computed ground-state structures for **5** and **6** closely matched the X-ray diffraction structures. Initial formation of **5** presumably results from addition of a putative 16-electron “Re(CO)₃(thpymS)” fragment to the triruthenium centre *via* insertion into the rhenium–sulphur bond. While the nature of the cluster isomerisation is not fully understood at this time, a plausible route is shown in Scheme 4. Here initial cleavage of the rhenium–nitrogen bond leads to a decrease in the skeletal electrons from 7 SEP to 6 SEP, and this is compensated by the formation of a new Ru–Re bond as the molecular polyhedron undergoes an arachno-to-nido transformation [47]. Accompanying this reaction is the formation of a bridging CO group at the new metal–metal bond. Subsequent rotation about the sulphur–carbon bond (or proton transfer between nitrogen atoms), followed by coordination of nitrogen to the initial wingtip ruthenium results and cleavage of this newly formed Ru–Re bond and concomitant migration of the transient μ₂-CO group to the



Scheme 3. Reaction of Re₂(CO)₆(μ-thpymS)₂ (**1**) with Ru₃(CO)₁₂.

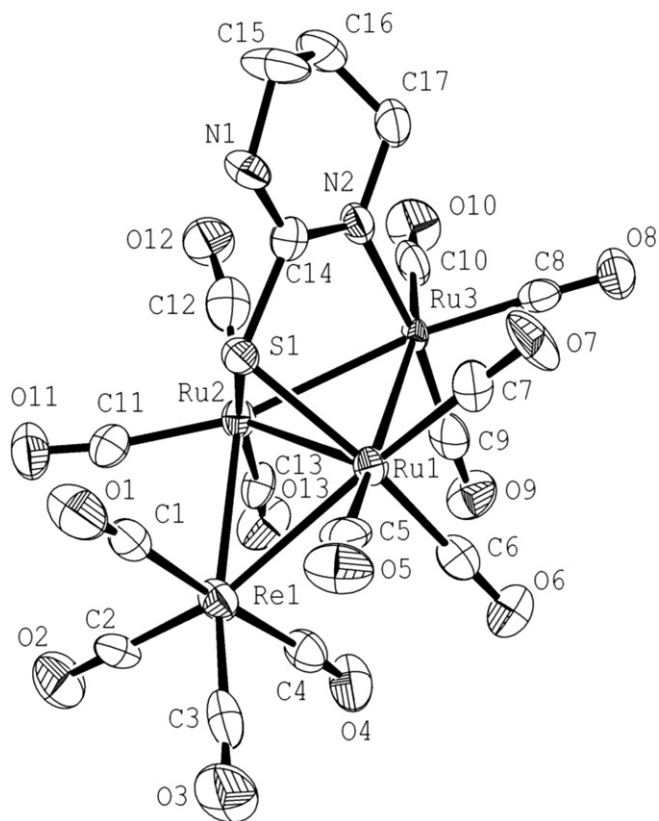
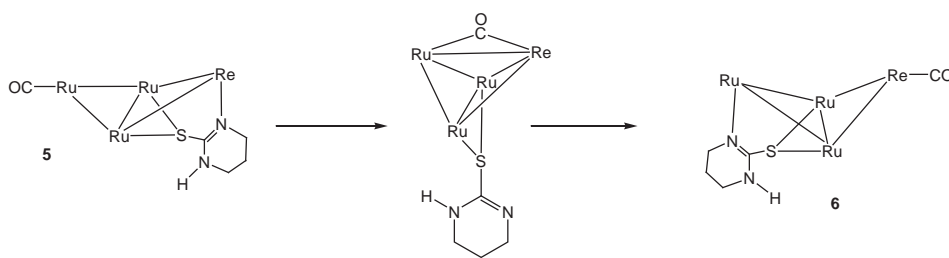


Fig. 3. X-ray structure of $\text{ReRu}_3(\text{CO})_{13}(\mu_3\text{-thpymS})$ (**6**) showing the atom labelling scheme used. The hydrogen atoms are omitted for clarity. Thermal ellipsoids are drawn at 50% probability level. Selected interatomic distances (Å) and angles ($^\circ$): Ru(1)–Ru(2) 2.786(1), Ru(1)–Ru(3) 2.819(1), Ru(2)–Ru(3) 2.832(1), Re(1)–Ru(1) 2.898(1), Re(1)–Ru(2) 2.920(1), Ru(3)–N(2) 2.16(1), Ru(1)–S(1) 2.372(3), Ru(2)–S(1) 2.371(3), Ru(1)–Re(1)–Ru(2) 57.22(3), N(2)–Ru(3)–Ru(1) 87.9(3), N(2)–Ru(3)–Ru(2) 86.6(3), Ru(1)–Ru(3)–Ru(2) 59.07(4), S(1)–Ru(1)–Ru(2) 54.02(8), S(1)–Ru(1)–Ru(3) 80.44(8), Ru(2)–Ru(1)–Ru(3) 60.69(4), S(1)–Ru(1)–Re(1) 82.93(8), Ru(2)–Ru(1)–Re(1) 61.79(3), Ru(3)–Ru(1)–Re(1) 118.61(4), S(1)–Ru(2)–Ru(1) 54.05(8), Ru(1)–Ru(2)–Ru(3) 60.24(4), S(1)–Ru(2)–Ru(3) 80.18(8), S(1)–Ru(2)–Re(1) 82.46(8), Ru(1)–Ru(2)–Re(1) 60.99(3), Ru(3)–Ru(2)–Re(1) 117.45(4), Ru(2)–S(1)–Ru(1) 71.93(9).

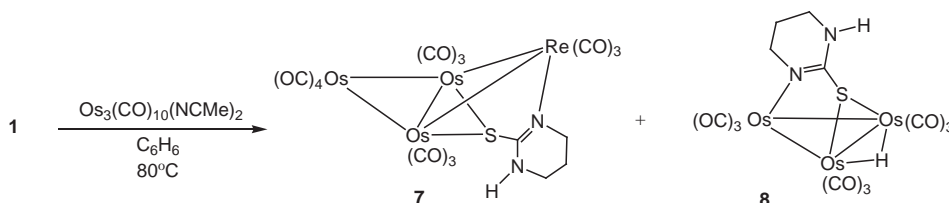
rhenium, completes the formal transfer of the face-capping tetrahydropyrimidine-2-thiolato ligand to the Ru_3 face. Such a process is attractive since the intermediate is an electron-precise tetrahedral cluster (60 valence electrons) and might thus be expected to provide a relatively low energy pathway.

A similar reaction between **1** and $\text{Os}_3(\text{CO})_{10}(\text{NCMe})_2$ gave $\text{Os}_3\text{Re}(\text{CO})_{13}(\mu_3\text{-thpymS})$ (**7**) as major product (45%) together with $\text{Os}_3(\text{CO})_9(\mu_3\text{-thpymS})(\mu\text{-H})$ (**8**) (8%) (Scheme 5). Cluster **7** was characterized by comparing its IR spectrum with that of **5**, specifically the highest frequency carbonyl vibration at 2107 cm^{-1} is consistent with that found in **5** (2101 cm^{-1}) but not **6** (2092 cm^{-1}). The FAB mass spectrum shows a parent molecular ion at m/z 1236 together with ions due to the successive loss of 13 carbonyls. The ^1H NMR spectrum displays three multiplets δ 4.23, 3.35, 1.98 (each integrating to 2H) and a broad singlet at δ 6.62 (integrating to 1H) assigned to the methylene and N–H protons of the pyrimidine-2-thiolato ligand.

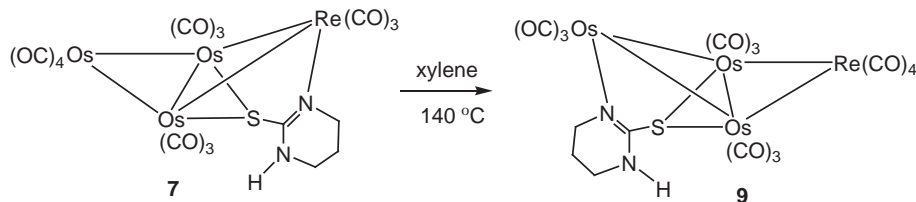
Under the reaction conditions described above (refluxing benzene), a second isomer of **7** was not observed and even when we heated **7** in toluene for a prolonged period this was also the case. However, in xylene the slow transformation of **7** was observed. Thus, heating for 1 h led to the loss of ca. 90% of **7** and formation of isomeric **9** in low (6.5%) yield (Scheme 6). DFT calculations were performed on **7** and **9**, and the latter cluster was found to lie 1.5 kcal mol^{-1} lower in energy, paralleling the trend found in clusters **5** and **6**. Given the favourable thermodynamics for the formation of cluster **9**, the observed decomposition that accompanies this isomerization reflects the higher activation barrier for the isomerization in the ReOs_3 system. Importantly trinuclear **8** was not generated under these conditions. Due to the small amounts of **9**, characterization was made on the basis of IR spectroscopy and elemental analysis with the former being quite distinct from that of **7**. The high temperature, low yield isomerisation of **7** to **9** is in contrast to that noted for the analogous Ru_3Re system. Presumably the nature of the rhenium–nitrogen bond in **7** is very similar to that in **5**, likewise formation of a new osmium–rhenium bond should also be favourable. It is well-known that carbonyl bridging across bonds between the heavier transition elements is not favoured and thus we suggest that it may be for this reason that isomerisation is not facile in this case [48].



Scheme 4. A plausible pathway for the isomerisation of **5** to **6**.



Scheme 5. Reaction of $\text{Re}_2(\text{CO})_6(\mu\text{-thpymS})_2$ (**1**) with $\text{Os}_3(\text{CO})_{10}(\text{NCMe})_2$.



Scheme 6. Isomerisation of $\text{Os}_3\text{Re}(\text{CO})_{13}(\mu_3\text{-thpymS})$ (**7**) to **9** upon heating in xylene.

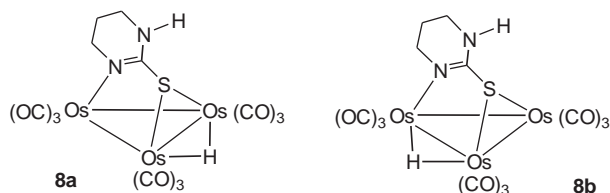


Chart 1. Two isomers of $\text{Os}_3(\text{CO})_9(\mu_3\text{-thpymS})(\mu\text{-H})$ (**8**).

The second product of the reaction, namely **8**, results from complete transfer of the tetrahydropyrimidine-2-thiolato ligand from rhenium to osmium. Its identity is readily determined from the IR spectrum, the pattern of which closely resembles other $\text{Os}_3(\text{CO})_9(\mu_3\text{-L})(\mu\text{-H})$ complexes [31]. The FAB mass spectrum displays a parent ion at m/z 939 and further ions due to stepwise loss of nine carbonyls. The ^1H NMR shows two sets of resonances in 3:1 ratio indicating that **8** exists in two isomeric forms in solution (Chart 1). The isomerism in this type of cluster occurs due to disposition of the hydride ligand across different osmium–osmium edges and both isomeric forms have been structurally characterized for $\text{Os}_3(\text{CO})_9(\mu_3\text{-L})(\mu\text{-H})$ ($\mu\text{-H} = 2\text{-mercapto-1-methylimidazole}$) [31]. The relationship between **7** and **8** is unclear.

4. Summary and conclusions

The synthesis and reactivity of the dirhenium complex $\text{Re}_2(\text{CO})_6(\mu\text{-thpymS})_2$ (**2**) have been investigated. Reactions of thpymSH with either $\text{Re}_2(\text{CO})_8(\text{NCMe})_2$ or $\text{Re}_2(\text{CO})_{10}$ gives the expected dirhenium complex $\text{Re}_2(\text{CO})_6(\mu\text{-thpymS})_2$ (**1**) in moderate yields (32–34%) along with small amounts of *eq*- $\text{Re}_2(\text{CO})_9(\kappa^1\text{-S})\text{-SN}_2\text{C}_4\text{H}_8$ (**2**) (5–11%). Complex **2** is a rare example of dirhenium complex containing a κ^1 -thiolato ligand. Reactions of **1** with mono- and diphosphines result in cleavage of the Re–S bond producing mononuclear complexes. With Group 8 trinuclear carbonyls tetranuclear mixed-metal butterfly clusters result. In all these reactions complex **1** acts as a source of $\text{Re}(\text{CO})_3(\text{thpymS})$ fragment which is a common feature of $\text{M}_2(\text{CO})_6(\mu\text{-L})_2$ ($\text{M} = \text{Re}, \text{Mn}$; $\text{L} = \text{heterocyclic thiolato ligand}$) type complexes. The most important finding from this study is that here for the first time we have isolated and structurally characterized a new isomeric form of $\text{M}_3\text{M}'(\text{CO})_{13}(\mu_3\text{-thpymS})$ ($\text{M} = \text{Ru}, \text{Os}$; $\text{M}' = \text{Mn}, \text{Re}$) type mixed-metal complexes, i.e., cluster **6** which is formed from **5** via transfer of nitrogen from rhenium to ruthenium with concomitant carbonyl migration. DFT calculations indicate that **6** is thermodynamically more stable by around 2 kcal mol^{-1} and a mechanism is proposed in which the pyrimidine-2-thiolato ligand becomes bidentate, the consequent loss of two electrons being compensated for by the formation of a new metal–metal bond. The corresponding osmium chemistry is less clean and along with the target cluster $\text{Os}_3\text{Re}(\text{CO})_{13}(\mu_3\text{-thpymS})$ (**7**), reaction of **1** with $\text{Os}_3(\text{CO})_{10}(\text{MeCN})_2$ also gave significant amounts of trinuclear $\text{Os}_3(\text{CO})_9(\mu_3\text{-thpymS})(\mu\text{-H})$ (**8**), in which the pyrimidine-2-thiolato ligand has been transmetallated.

Cluster **7** is stable in both refluxing benzene and toluene but in xylene at 140°C it slowly converts into isomeric **9**, although yields are poor due to accompanying decomposition. The reason(s) for this reactivity difference between the Ru_3Re and ReOs_3 clusters is not fully understood but we speculate that the isomerism proceeds via an intermediate containing a bridging carbonyl and such species are known to be unfavourable across metal–metal bonds formed from the heavier transition elements.

Acknowledgements

This research has been jointly sponsored by the Ministry of Science and Information & Communication Technology and Ministry of Education, Government of the People's Republic of Bangladesh. We thank the Commonwealth Scholarship Commission for the award of a Commonwealth Scholarship to SG. Financial support from the Robert A. Welch Foundation (Grant B-1093-MGR) and the NSF (CHE-0741936) is acknowledged and we would like to thank the Title-III fund of the US Department of Education for providing support for the purchase of the diffractometer at Tennessee State University.

Appendix A. Supplementary material

CCDC 880835 for **3**, CCDC 880834 for **5** and CCDC 890659 for **6** contain supplementary crystallographic data for this paper. These data may be obtained free of charge from The Cambridge Crystallographic Data Center via www.ccdc.cam.ac.uk/data_request/cif. Atomic coordinates and DFT-computed energies for clusters **5**, **6**, **7**, and **9** are available from MGR upon request.

References

- [1] S.G. Rosenfield, H.P. Berends, L. Gelmini, D.W. Stephan, P.K. Mascharak, *Inorg. Chem.* 26 (1987) 2792.
- [2] R. Castro, M.L. Durán, J.A. Garcia-Vázquez, J. Romero, A. Sousa, A. Castiñeiras, W. Hiller, J. Strähle, *J. Chem. Soc. Dalton Trans.* (1990) 531.
- [3] C.O. Kienitz, C. Thöne, P. Jones, *Inorg. Chem.* 35 (1996) 3990.
- [4] A.J. Deeming, M. Karim, P.A. Bates, M.B. Hursthouse, *Polyhedron* 7 (1988) 1401.
- [5] D. Katiyar, V.K. Tiwari, R.P. Tripathi, A. Srivastava, V. Chaturvedi, R. Srivastava, B.S. Srivastava, *Bioorg. Med. Chem.* 11 (2003) 4369.
- [6] M. Berardini, J. Brennan, *Inorg. Chem.* 34 (1995) 6179.
- [7] D.J. Rose, Y.D. Chang, Q. Chen, P.B. Kettler, J. Zubieta, *Inorg. Chem.* 34 (1995) 3973.
- [8] Y. Cheng, T.J. Emge, J.G. Brennan, *Inorg. Chem.* 35 (1996) 342.
- [9] J. Lee, T.J. Emge, J.G. Brennan, *Inorg. Chem.* 36 (1997) 5064.
- [10] A.J. Deeming, M. Karim, N.I. Powell, K.I. Hardcastle, *Polyhedron* 9 (1990) 623.
- [11] B. Cockerton, A.J. Deeming, M. Karim, K.I. Hardcastle, *J. Chem. Soc. Dalton Trans.* (1991) 431.
- [12] N. Lugin, J.J. Bonnet, J.A. Ibers, *J. Am. Chem. Soc.* 107 (1985) 4484.
- [13] N. Choi, G. Conole, M. Kessler, J.D. King, M.J. Mays, M. McPartlin, G.E. Pateman, G.A. Solan, *J. Chem. Soc. Dalton Trans.* (1999) 3941.
- [14] B.F.G. Johnson, J. Lewis, D.A. Pippard, *J. Chem. Soc. Dalton Trans.* (1981) 407.
- [15] S.E. Kabir, M.R. Hassan, D.T. Haworth, S.V. Lindeman, T.A. Siddiquee, D.W. Bennett, *J. Organomet. Chem.* 692 (2007) 3936.
- [16] S.E. Kabir, G. Hogarth, *Coord. Chem. Rev.* 253 (2009) 1285.
- [17] M.A. Mottalib, S.E. Kabir, D.A. Tocher, A.J. Deeming, E. Nordlander, *J. Organomet. Chem.* 692 (2007) 5007.

- [18] S. Ghosh, S.E. Kabir, S. Pervin, G.M.G. Hossain, D.T. Haworth, S.V. Lindeman, T.A. Siddiquee, D.W. Bennett, H.W. Roesky, Z. Anorg. Allg. Chem. 635 (2009) 76.
- [19] S. Ghosh, S.E. Kabir, S. Pervin, A.K. Raha, G.M.G. Hossain, D.T. Haworth, S.V. Lindeman, D.W. Bennett, T.A. Siddiquee, L. Salassa, H.W. Roesky, J. Chem. Soc. Dalton Trans. (2009) 3510.
- [20] S. Ghosh, K.N. Khanam, G.M.G. Hossain, D.T. Haworth, S.V. Lindeman, G. Hogarth, S.E. Kabir, New J. Chem. 34 (2010) 1875.
- [21] S.G. Rosenfield, S.A. Swedberg, S.K. Arora, P.K. Mascharak, Inorg. Chem. 25 (1986) 2109.
- [22] A.J. Deeming, K.I. Hardcastle, M.N. Meah, P.A. Bates, H.M. Dawes, M.B. Hursthouse, J. Chem. Soc. Dalton Trans. (1988) 227.
- [23] A.J. Deeming, M. Karim, N.I. Powell, J. Chem. Soc. Dalton Trans. (1990) 2321.
- [24] D.J. Rose, Y.D. Chang, Q. Chen, J. Zubietta, Inorg. Chem. 23 (1994) 5167.
- [25] S. Kitagawa, M. Munakata, H. Shimonono, S. Matsuyama, S. Masuda, J. Chem. Soc. Dalton Trans. (1990) 2105.
- [26] S.E. Kabir, M.M. Karim, K. Kundu, S.M.B. Ullah, K.I. Hardcastle, J. Organomet. Chem. 517 (1996) 155.
- [27] M. Islam, C.A. Johns, S.E. Kabir, K. Kundu, K.M.A. Malik, S.M.B. Ullah, J. Chem. Crystallogr. 29 (1999) 1001.
- [28] S. Ghosh, K.N. Khanam, M.K. Hossain, G.M.G. Hossain, D.T. Haworth, S.V. Lindeman, G. Hogarth, S.E. Kabir, J. Organomet. Chem. 695 (2010) 1146.
- [29] S. Ghosh, F.K. Camellia, K. Fatema, M.I. Hossain, M.R. Al-Mamum, G.M.G. Hossain, G. Hogarth, S.E. Kabir, J. Organomet. Chem. 696 (2011) 2935.
- [30] S. Ghosh, F. Ahmed, R. Al-Mamun, D.T. Haworth, S.V. Lindeman, T.A. Siddiquee, D.W. Bennett, S.E. Kabir, J. Chem. Crystallogr. 39 (2009) 595.
- [31] S. Ghosh, S.E. Kabir, M. Khatun, D.T. Haworth, S.V. Lindeman, T.A. Siddiquee, D.W. Bennett, J. Chem. Crystallogr. 39 (2009) 632.
- [32] S.E. Kabir, J. Alam, S. Ghosh, K. Kundu, G. Hogarth, D.A. Tocher, G.M.G. Hossain, H.W. Roesky, J. Chem. Soc. Dalton Trans. (2009) 4458.
- [33] K.A. Azam, K.M. Hanif, A.C. Ghosh, S.E. Kabir, S.R. Kamakar, K.M.A. Malik, S. Parvin, E. Rosenberg, Polyhedron 21 (2002) 885.
- [34] S. Ghosh, M.S.A. Mia, E. Begum, G.M.G. Hossain, Inorg. Chim. Acta 384 (2012) 76–82.
- [35] M.S. Rahman, J.C. Sarker, S. Ghosh, S.E. Kabir, Aust. J. Chem. 65 (2012) 796.
- [36] M.A. Khaleque, K.A. Azam, M.M. Karim, S. Ghosh, G. Hogarth, S.E. Kabir, Aust. J. Chem. 65 (2012) 773.
- [37] W.L. Ingham, N.J. Coville, J. Organomet. Chem. 423 (1992) 51.
- [38] L.J. Farrugia, J. Appl. Crystallogr. 32 (1999) 837.
- [39] N. Walker, D. Stuart, Acta Crystallogr. A39 (1983) 158.
- [40] G.M. Sheldrick, Acta Crystallogr. Sect. A46 (1990) 467.
- [41] G.M. Sheldrick, SHELXL-97 Program for Crystal Structure Refinement, Göttingen University, Germany, 1997.
- [42] M.J. Frisch, et al., Gaussian 09, Revision A.02, Gaussian, Inc., Wallingford CT, 2009.
- [43] A.D. Becke, J. Chem. Phys. 98 (1993) 5648.
- [44] C. Lee, W. Yang, R.G. Parr, Phys. Rev. B37 (1988) 785.
- [45] H. Alper, Inorg. Chem. 15 (1976) 962.
- [46] S. Ghosh, G.M.G. Hossain, S.E. Kabir, J. Bangladesh Chem. Soc., in press.
- [47] For related examples involving similar phenomena, see: (a) K. Wade, in: B.F.G. Johnson (Ed.), Transition Metal Clusters, Wiley, Chichester, England, 1980 [Chapter 3]; (b) V.J. Johnston, F.W.B. Einstein, R.K. Pomeroy, Organometallics 7 (1988) 1867; (c) P. Braunstein, C. de Méric de Bellefon, S.-E. Bouaoud, D. Grandjean, J.-F. Halet, J.-Y. Saillard, J. Am. Chem. Soc. 113 (1991) 5282; (d) B. Xu, Q.-S. Li, Y. Xie, R.B. King, H.F. Schaefer III, Dalton Trans. (2008) 1366.
- [48] (a) P.J. Dyson, J.S. McIndoe, Transition Metal Carbonyl Cluster Chemistry, Gordon and Breach Publishers, Amsterdam, NL, 2000; (b) A.K. Hughes, K. Wade, Coord. Chem. Rev. 197 (2000) 191.